PHYSICAL REVIEW D **71,** 115001 (2005)

Deconstructed Higgsless models with one-site delocalization

R. Sekhar Chivukula* and Elizabeth H. Simmons†
Department of Physics and Astronomy, Michigan State University, East Lansing, Michigan 48824, USA

Hong-Jian He‡
Department of Physics, University of Texas, Austin, Texas 78712 USA

Masafumi Kurachi§
Department of Physics, Nagoya University, Nagoya 464-8602, Japan
Department of Physics, Tohoku University, Sendai 980-8578, Japan

Masaharu Tanabashi‖
Department of Physics, Tohoku University, Sendai 980-8578, Japan
(Received 24 February 2005; published 3 June 2005)

In this note we calculate the form of electroweak corrections in deconstructed Higgsless models for the case of a fermion whose weak properties arise from two adjacent $SU(2)$ groups on the deconstructed lattice. We show that, as recently proposed in the continuum, it is possible for the value of the electroweak parameter αS to be small in such a model. In addition, by working in the deconstructed limit, we may directly evaluate the size of off-Z-pole electroweak corrections arising from the exchange of Kaluza-Klein modes; this has not been studied in the continuum. The size of these corrections is summarized by the electroweak parameter $\alpha\delta$. In one-site delocalized Higgsless models with small values of αS, we show that the amount of delocalization is bounded from above, and must be less than 25% at 95% C.L. We discuss the relation of these calculations to our previous calculations in deconstructed Higgsless models, and to models of extended technicolor. We present numerical results for a four-site model, illustrating our analytic calculations.

DOI: 10.1103/PhysRevD.71.115001 PACS numbers: 12.60.Fr

I. INTRODUCTION

"Higgsless" models [1] have emerged as an intriguing direction for research into the origin of electroweak symmetry breaking. In these models, which are based on five-dimensional gauge theories compactified on an interval, unitarization of the electroweak bosons' self-interactions occurs through the exchange of a tower of massive vector bosons [2–5], rather than the exchange of a scalar Higgs boson [6].

We have recently analyzed the electroweak corrections in a large class of Higgsless models in which the fermions are localized within the extra dimension [7–9]. Specifically, we studied all Higgsless models which can be deconstructed [10,11] to a chain of $SU(2)$ gauge groups adjacent to a chain of $U(1)$ gauge groups, with the fermions coupled to any single $SU(2)$ group and to any single $U(1)$ group along the chain. Our use of deconstruction allowed us to relate the size of corrections to electroweak processes directly to the spectrum of vector bosons ["Kaluza-Klein (KK) modes"] which, in Higgsless models, is constrained by unitarity. Our results apply for arbitrary background 5D geometry, spatially dependent gauge couplings, and brane kinetic energy terms.

We found [7] that Higgsless models with localized fermions which do not have extra light vector bosons (with masses of order the W and Z masses) cannot simultaneously satisfy the constraints of precision electroweak data and unitarity bounds. In particular, we found that unitarity constrains the electroweak parameter $\hat{S}$ as follows:

$$\hat{S} = \frac{1}{4s^2}\left(\alpha S + 4c^2(\Delta\rho - \alpha T) + \frac{\alpha\delta}{c^2}\right) \geq M_W^2 \Sigma_r \geq \frac{M_W^2}{8\pi v^2} \simeq 4 \times 10^{-3}. \tag{1.1}$$

This large a value is disfavored by precision electroweak data [12].

Although we framed those results in terms of their application to continuum Higgsless 5D models, they also apply far from the continuum limit when only a few extra vector bosons are present. As such, these results form a generalization of phenomenological analyses [13] of models of extended electroweak gauge symmetries [14–16] motivated by models of hidden local symmetry [17–21]. Our previous results are complementary to, and more general than, the analyses of the phenomenology of these

*Electronic address: sekhar@msu.edu
†Electronic address: esimmons@msu.edu
‡Electronic address: hjhe@physics.utexas.edu
§Electronic address: kurachi@tuhep.phys.tohoku.ac.jp
‖Electronic address: tanabash@tuhep.phys.tohoku.ac.jp

models in the continuum [12,22–29]. They also apply independent of the form of the high-energy completion of the Higgsless theory; the potentially large higher-order corrections expected to be present in QCD-like completions have been discussed in [30].

It has been proposed [31,32] that the size of corrections to electroweak processes may be reduced by allowing for delocalized fermions. We now investigate this possibility in the context of deconstruction. This paper will focus on the effects of adding fermion delocalization to the deconstructed models which our earlier work identified as having the greatest phenomenological promise (i.e., those in which the electroweak corrections are smallest). These are models (designated "case I") in which the fermions' hypercharge interactions are with the $U(1)$ group at the interface between the $SU(2)$ and $U(1)$ groups, and in which the gauge couplings of that $U(1)$ group and of the $SU(2)$ group farthest from the interface are small. For simplicity, we will assume, in this paper, that the $U(1)$ group adjacent to the interface is the only hypercharge group in the model; this corresponds to taking the $M = 0$ limit of the more general models we studied previously [7]. We also assume that the fermions derive their weak properties from two adjacent $SU(2)$ groups in the deconstructed model—i.e., we consider "one-site" delocalization.

We have found several relationships between delocalization and electroweak corrections, some confirming what has been found in the continuum and others entirely new. We confirm that it is possible for the value of the electroweak parameter αS to be small in models including fermion delocalization; this has been shown already in the continuum [31,32]. By working in the deconstructed limit, we may directly evaluate the size of electroweak corrections away from the Z peak which arise from the exchange of Kaluza-Klein modes; this has not previously been examined in the continuum. The size of these corrections is summarized by the electroweak parameter $\alpha\delta$ [9,12], which describes flavor-universal nonoblique corrections. In one-site delocalized Higgsless models with small values of αS, we show that the amount of delocalization is bounded from above by a combination of experimental limits on $\alpha\delta$ and the need to ensure that the scattering of longitudinal W bosons is properly unitarized. At 95% C.L., the amount of delocalization cannot exceed 25%. We discuss the relation of these calculations to our previous calculations in deconstructed Higgsless models, and to models of extended technicolor. We defer to a subsequent work [33,34] the study of multisite or flavor nonuniversal delocalization, and the generation of fermion masses.[1]

In the next two sections we discuss the structure of the gauge and fermion sectors of the model, and specify the limit in which we analytically compute the size of corrections to electroweak interactions. In Secs. IV, V, and VI, we compute the electroweak parameters αS, αT, and $\alpha\delta$, respectively.[2] In Sec. VII we discuss the interpretation of these models, and discuss how such effects can arise in technicolor theories. In Sec. VIII we present numerical results for a four-site model, illustrating our analytic calculations and demonstrating explicitly that some models with vanishing αS can have relatively large values of $\alpha\delta$. Section IX discusses our conclusions and outlines future work.

II. REVIEW OF THE GAUGE SECTOR OF THE MODEL

We study a deconstructed Higgsless model, as shown diagrammatically (using "moose notation" [35]) in Fig. 1. The model incorporates an $SU(2)^{N+1} \times U(1)$ gauge group, and $N + 1$ nonlinear $(SU(2) \times SU(2))/SU(2)$ sigma models in which the global symmetry groups in adjacent sigma models are identified with the corresponding factors of the gauge group. The Lagrangian for this model to leading order is given by

$$\mathcal{L}_2 = \frac{1}{4}\sum_{j=1}^{N+1} f_j^2 \mathrm{tr}((D_\mu U_j)^\dagger (D^\mu U_j)) - \sum_{j=0}^{N+1} \frac{1}{2g_j^2}\mathrm{tr}(F^j_{\mu\nu}F^{j\mu\nu}), \tag{2.1}$$

with

$$D_\mu U_j = \partial_\mu U_j - iA^{j-1}_\mu U_j + iU_j A^j_\mu, \tag{2.2}$$

where all gauge fields A^j_μ $(j = 0, 1, 2, \ldots, N + 1)$ are dynamical. The first $N + 1$ gauge fields $(j = 0, 1, \ldots, N)$ correspond to $SU(2)$ gauge groups; the last gauge field $(j = N + 1)$ corresponds to the $U(1)$ gauge group. The symmetry breaking between the A^N_μ and A^{N+1}_μ follows an $SU(2)_L \times SU(2)_R/SU(2)_V$ symmetry breaking pattern with the $U(1)$ embedded as the T_3 generator of $SU(2)_R$. Our analysis proceeds for arbitrary values of the gauge couplings and f constants, and therefore allows for arbitrary background 5D geometry, spatially dependent gauge couplings, and brane kinetic energy terms for the gauge bosons.

All four-fermion processes, including those relevant for the electroweak phenomenology of our model, depend on the neutral and charged gauge field propagator matrices

$$\begin{aligned} D^Z(Q^2) &\equiv [Q^2\mathcal{I} + M_Z^2]^{-1}, \\ D^W(Q^2) &\equiv [Q^2\mathcal{I} + M_W^2]^{-1}. \end{aligned} \tag{2.3}$$

Here, M_Z^2 and M_W^2 are, respectively, the mass-squared matrices for the neutral and charged gauge bosons and $\mathcal{I}$ is the identity matrix. Consistent with [8], $Q^2 \equiv -q^2$ refers to the Euclidean momentum.

[1]Flavor nonuniversal interactions will be required in order to generate the diverse fermion masses. Depending on how this is done, these new interactions may lead to additional flavor nonuniversal electroweak corrections [31].

[2]The fourth such parameter, $\Delta\rho$, is identically equal to 0 in case I models [7].

The neutral vector meson mass-squared matrix is of dimension $(N+2)\times(N+2)$

$$M_Z^2 = \frac{1}{4}\begin{pmatrix} g_0^2 f_1^2 & -g_0 g_1 f_1^2 & & & \\ -g_0 g_1 f_1^2 & g_1^2(f_1^2+f_2^2) & -g_1 g_2 f_2^2 & & \\ & \ddots & \ddots & \ddots & \\ & & -g_{N-1}g_N f_N^2 & g_N^2(f_N^2+f_{N+1}^2) & -g_N g_{N+1} f_{N+1}^2 \\ & & & -g_N g_{N+1} f_{N+1}^2 & g_{N+1}^2 f_{N+1}^2 \end{pmatrix}, \tag{2.4}$$

and the charged-current vector bosons' mass-squared matrix is the left-upper $(N+1)\times(N+1)$ dimensional block of the neutral-current M_Z^2 matrix. The neutral mass matrix (2.4) is of a familiar form that has a vanishing determinant, due to a zero eigenvalue. Physically, this corresponds to a massless neutral gauge field—the photon. The nonzero eigenvalues of M_Z^2 are labeled by m_{Zz}^2 ($z = 0, 1, 2, \ldots, N$), while those of M_W^2 are labeled by m_{Ww}^2 ($w = 0, 1, 2, \ldots, N$). The lowest massive eigenstates corresponding to eigenvalues m_{Z0}^2 and m_{W0}^2 are, respectively, identified as the usual Z and W bosons. We will generally refer to these last eigenvalues by their conventional symbols M_Z^2, M_W^2; the distinction between these and the corresponding mass matrices should be clear from the context.

Generalizing the usual mathematical notation for "open" and "closed" intervals, we may denote [7] the neutral-boson mass matrix M_Z^2 as $M_{[0,N+1]}^2$—i.e., it is the mass matrix for the entire moose running from site 0 to site $N+1$ including the gauge couplings of both endpoint groups. Analogously, the charged-boson mass matrix M_W^2 is $M_{[0,N+1)}^2$—it is the mass matrix for the moose running from site 0 to link $N+1$, but not including the gauge coupling at site $N+1$. This notation will be useful in thinking about the properties of submatrices $M_{[0,i)}^2$ of the full gauge-boson mass matrices that arise in our discussion of fermion delocalization, and also the corresponding eigenvalues $m_{i\hat{i}}^2$ ($\hat{i} = 1, 2, \ldots, i$). We will denote the lightest such eigenvalue m_{i1}^2 by the symbol M_i^2.

III. A MOOSE WITH DELOCALIZED FERMIONS

Consider the simplest deconstructed Higgsless model with one-site delocalized fermions, as shown in Fig. 1. We take the fermion couplings in this model to be

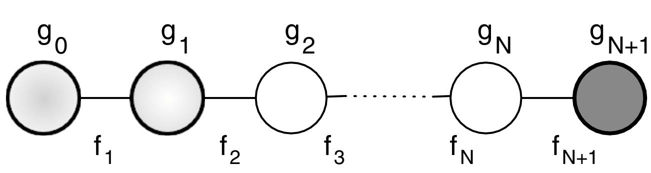

FIG. 1. Moose diagram of the model analyzed in this paper. Sites 0 to N are $SU(2)$ gauge groups, site $N+1$ is a $U(1)$ gauge group. The fermions are one-site-delocalized in the sense that the $SU(2)$ couplings of the fermions arise from the gauge groups at sites 0 and 1. The $U(1)$ coupling comes from the gauge group at site $N+1$.

$$\mathcal{L}_f = \vec{J}_L^\mu \cdot (x_0 A_\mu^0 + x_1 A_\mu^1) + J_Y^\mu A_\mu^{N+1}, \tag{3.1}$$

where $x_0 + x_1 = 1$ and the fermions are "delocalized" in the sense that their $SU(2)$ couplings arise from both sites 0 and 1. Note that the fermion couplings are flavor universal. This expression is not separately gauge invariant under $SU(2)_0$ and $SU(2)_1$. Rather, as discussed further in Sec. VII, Eq. (3.1) should be viewed as the form of the fermion coupling in "unitary" gauge. Here $\vec{J}_L^\mu$ denotes the isotriplet of left-handed weak fermion currents, and J_Y^μ is the fermion hypercharge current. In the notation of Ref. [7], where the fermion coupled to the $SU(2)$ group at site p, the current model is an admixture of $p = 0$ and $p = 1$. As we will see, our results for the electroweak parameters in this model are themselves an admixture of the results we would obtain in the two models.[3]

Because fermions are charged under $SU(2)$ gauge groups at sites 0 and 1, as well as under the single $U(1)$ group at the $N+1$ site, neutral-current four-fermion processes may be derived from the Lagrangian

$$\begin{aligned} \mathcal{L}_{NC} = &-\frac{1}{2}\Big[\sum_{i,j=0}^{1} x_i x_j g_i g_j D_{i,j}^Z(Q^2)\Big] J_3^\mu J_{3\mu} \\ &- \Big[\sum_{i=0}^{1} x_i g_i g_{N+1} D_{i,N+1}^Z(Q^2)\Big] J_3^\mu J_{Y\mu} \\ &- \frac{1}{2}[g_{N+1}^2 D_{N+1,N+1}^Z(Q^2)] J_Y^\mu J_{Y\mu}, \end{aligned} \tag{3.2}$$

and the charged-current process from

$$\mathcal{L}_{CC} = -\frac{1}{2}\Big[\sum_{i,j=0}^{1} x_i x_j g_i g_j D_{i,j}^W(Q^2)\Big] J_+^\mu J_{-\mu}, \tag{3.3}$$

where $D_{i,j}$ is the (i, j) element of the appropriate gauge field propagator matrix. We can define correlation functions between fermion currents at given sites as

$$\begin{aligned} [G_{NC}(Q^2)]_{i,j} &= g_i g_j D_{i,j}^Z(Q^2) \\ [G_{CC}(Q^2)]_{i,j} &= g_i g_j D_{i,j}^W(Q^2). \end{aligned} \tag{3.4}$$

[3]The idea of a delocalized model as an admixture of localized-fermion models corresponding to different values of p generalizes readily to multisite delocalization. The generalization of the form of Eqs. (3.1), (3.2), (3.3), (3.4), (3.5), (3.6), and (3.7) is obvious; the implications will be discussed in a forthcoming paper [34].

The full correlation function for the fermion currents J_3^μ and J_Y^μ is then

$$[G_{NC}(Q^2)]_{WY} = \sum_{i=0}^{1} x_i [G_{NC}(Q^2)]_{i,N+1}, \tag{3.5}$$

where we have used Eq. (3.1) to include the appropriate contribution from each site to which fermions couple. Likewise, the full correlation function for weak currents is

$$[G_{NC,CC}]_{WW} = \sum_{i,j=0}^{1} x_i x_j [G_{NC,CC}]_{i,j}. \tag{3.6}$$

The hypercharge correlation function $[G_{NC}(Q^2)]_{YY} = [G_{NC}(Q^2)]_{N+1,N+1}$ depends only on the single site with a $U(1)$ gauge group.

The correlation functions may be written in a spectral decomposition in terms of the mass eigenstates as follows:

$$[G_{NC}(Q^2)]_{YY} = \frac{[\xi_\gamma]_{YY}}{Q^2} + \frac{[\xi_Z]_{YY}}{Q^2 + M_Z^2} + \sum_{z=1}^{N} \frac{[\xi_{Zz}]_{YY}}{Q^2 + \mathsf{m}_{Zz}^2}, \tag{3.7}$$

$$[G_{NC}(Q^2)]_{WY} = \frac{[\xi_\gamma]_{WY}}{Q^2} + \frac{[\xi_Z]_{WY}}{Q^2 + M_Z^2} + \sum_{z=1}^{N} \frac{[\xi_{Zz}]_{WY}}{Q^2 + \mathsf{m}_{Zz}^2}, \tag{3.8}$$

$$[G_{NC}(Q^2)]_{WW} = \frac{[\xi_\gamma]_{WW}}{Q^2} + \frac{[\xi_Z]_{WW}}{Q^2 + M_Z^2} + \sum_{z=1}^{N} \frac{[\xi_{Zz}]_{WW}}{Q^2 + \mathsf{m}_{Zz}^2}, \tag{3.9}$$

$$[G_{CC}(Q^2)]_{WW} = \frac{[\xi_W]_{WW}}{Q^2 + M_W^2} + \sum_{w=1}^{N} \frac{[\xi_{Ww}]_{WW}}{Q^2 + \mathsf{m}_{Ww}^2}. \tag{3.10}$$

All poles should be simple (i.e. there should be no degenerate mass eigenvalues) because, in the continuum limit, we are analyzing a self-adjoint operator on a finite interval. Since the neutral bosons couple to only two currents, J_3^μ and J_Y^μ, the three sets of residues in Eqs. (3.7), (3.8), and (3.9) must be related. Specifically, they satisfy the $N+1$ consistency conditions,

$$\begin{aligned} [\xi_Z]_{WW}[\xi_Z]_{YY} &= ([\xi_Z]_{WY})^2, \\ [\xi_{Zz}]_{WW}[\xi_{Zz}]_{YY} &= ([\xi_{Zz}]_{WY})^2. \end{aligned} \tag{3.11}$$

In the case of the photon, charge universality further implies

$$e^2 = [\xi_\gamma]_{WW} = [\xi_\gamma]_{WY} = [\xi_\gamma]_{YY}. \tag{3.12}$$

A. Notation

We will find it useful to define the following sums over heavy eigenvalues for phenomenological discussions:

$$\Sigma_{(i,j)} \equiv \mathrm{Tr} M_{(i,j)}^{-2} \tag{3.13}$$

with similar definitions for $\Sigma_{[i,j)}$ and so on. In particular,

$$\Sigma_Z \equiv \sum_{z=1}^{N} \frac{1}{\mathsf{m}_{Zz}^2}, \qquad \Sigma_W \equiv \sum_{w=1}^{N} \frac{1}{\mathsf{m}_{Ww}^2}; \tag{3.14}$$

that is, Σ_Z and Σ_W are the sums over inverse-square masses of the higher neutral- and charged-current KK modes of the full model. Furthermore, by explicit calculation one finds (see Appendix B of Ref. [7])

$$\Sigma_{(0,N+1)} = \sum_{i=1}^{N} \frac{4F^2}{g_i^2 F_i^2 \tilde{F}_i^2}, \tag{3.15}$$

where

$$\frac{1}{F_i^2} = \sum_{j=i+1}^{N+1} \frac{1}{f_j^2}, \qquad \frac{1}{\tilde{F}_i^2} = \sum_{j=1}^{i} \frac{1}{f_j^2}, \tag{3.16}$$

and $F_0^2 = \tilde{F}_{N+1}^2 = F^2$.

Finally, we will find it useful to denote the (0,0) element of the gauge-boson mass matrices as

$$[M_Z^2]_{0,0} = [M_W^2]_{0,0} = \frac{g_0^2 f_1^2}{4} \equiv \tilde{\mathsf{m}}^2. \tag{3.17}$$

To connect with the notation of Ref. [7] we note that

$$\tilde{\mathsf{m}}^{-2} = \Sigma_{[0,1)} \equiv \Sigma_{p=1}. \tag{3.18}$$

B. Electroweak parameters

As we have shown in [9], the most general amplitude [to leading order in deviation from the standard model (SM)] for low-energy four-fermion neutral weak current processes in any "universal" model [12] may be written as[4]

$$\begin{aligned} -\mathcal{M}_{NC} = e^2 \frac{\mathcal{Q}\mathcal{Q}'}{Q^2} &+ \frac{(I_3 - s^2\mathcal{Q})(I_3' - s^2\mathcal{Q}')}{(\frac{s^2c^2}{e^2} - \frac{S}{16\pi})Q^2 + \frac{1}{4\sqrt{2}G_F}(1 - \alpha T + \frac{\alpha\delta}{4s^2c^2})} \\ &+ \sqrt{2}G_F \frac{\alpha\delta}{s^2c^2} I_3 I_3' + 4\sqrt{2}G_F(\Delta\rho - \alpha T) \\ &\times (\mathcal{Q} - I_3)(\mathcal{Q}' - I_3'), \end{aligned} \tag{3.19}$$

and the matrix element for the charged-current process may be written

[4] See [9] for a discussion of the correspondence between the "on-shell" parameters defined here, and the zero-momentum parameters defined in [12]. Note that U is shown in [9] to be zero to the order we consider in this paper.

$$-\mathcal{M}_{CC} = \frac{(I_+ I'_- + I_- I'_+)/2}{(\frac{s^2}{e^2} - \frac{S}{16\pi})Q^2 + \frac{1}{4\sqrt{2}G_F}(1 + \frac{\alpha\delta}{4s^2c^2})} + \sqrt{2}G_F \frac{\alpha\delta}{s^2c^2}\frac{(I_+ I'_- + I_- I'_+)}{2}. \qquad (3.20)$$

Note that the parameter s^2 is defined implicitly in these expressions as the ratio of the Q and I_3 couplings of the Z boson. S and T are the familiar oblique electroweak parameters [36–38], as determined by examining the *on-shell* properties of the Z and W bosons. $\Delta\rho$ corresponds to the deviation from unity of the ratio of the strengths of low-energy isotriplet weak neutral-current scattering and charged-current scattering. Finally, the contact interactions proportional to $\alpha\delta$ and $(\Delta\rho - \alpha T)$ correspond to ''universal nonoblique'' corrections.

From our previous analysis [7], we know that for a model of the sort shown in Fig. 1, $\Delta\rho \equiv 0$. In the limit in which we will work [see Eqs. (3.22) and (3.23)], we will also find (Sec. V) that $\alpha T \approx 0$. Therefore our analysis of electroweak corrections in these models reduces to computing the values of αS and $\alpha\delta$.

C. The limit taken

We will study the correlation functions for $0 \le -Q^2 \le (200\ \text{GeV})^2$ at tree level assuming that the heavy W and Z bosons satisfy

$$\mathsf{m}^2_{Zz}, \mathsf{m}^2_{Ww} \gg (200\ \text{GeV})^2, \qquad [z, w = 1, \ldots, N]. \qquad (3.21)$$

From our previous analysis [7], we expect that g_{N+1} [being the only $U(1)$ coupling] must be smaller than the other g_i in order to ensure that a light Z state will exist. In principle, any one of the $SU(2)$ couplings could also be small (to ensure the presence of a light W). However, our previous analysis [7] tells us that, in a viable model, any site with a small coupling must be linked by large f constants to site 0. For simplicity, we will therefore restrict our attention to the case where the only $SU(2)$ site with a small coupling is site 0. This may be viewed as analyzing the general model after having ''integrated out'' the links with large f constants.

In our analytic work, therefore, we will work in the limit that

$$g_0, g_{N+1} \ll g_i, \qquad i = 1, \ldots, N. \qquad (3.22)$$

From the analyses presented in [7], we find that in the limit of Eq. (3.22),

$$\Sigma_Z \approx \Sigma_W \approx \Sigma_{(0,N+1)} \equiv \Sigma_r, \qquad (3.23)$$

where the last definition makes contact with the notation $M^2_{(0,N+1)} \equiv M^2_r$ in Ref. [7], and

$$M_W^2 = \frac{g_0^2 F^2}{4} + \mathcal{O}\left(\frac{M_W^2}{\mathsf{m}^2_{W1}}\right). \qquad (3.24)$$

Note that we expect g_0 to be approximately of the order of the standard model $SU(2)$ coupling and therefore numerically of order 1—the limit in Eq. (3.22) implies that the other g_i will be larger, and Eq. (3.24) implies that $F \simeq 246$ GeV.

For phenomenologically motivated reasons [see Eq. (4.12)], we will also take

$$x_1 \frac{\{-Q^2, M_W^2\}}{\tilde{\mathsf{m}}^2} \ll 1. \qquad (3.25)$$

This approximation may be satisfied either by x_1 being small, $\tilde{\mathsf{m}}^2$ being large, or some combination thereof.

In the numerical examples studied in Sec. VIII, we calculate the tree-level masses and residues exactly, and we confirm that our analytic calculations based on the approximations of Eqs. (3.22) and (3.25) do indeed capture the essential features of models with one-site delocalization.

IV. $[G_{NC}(Q^2)]_{WY}$, $[\xi_Z]_{WY}$ AND αS

We begin by computing $[G_{NC}(Q^2)]_{WY}$. Starting from Eq. (3.5), we see the two contributions coming from the two sites at which the fermion resides. Based on Ref. [7], then, we may immediately compute the two relevant elements of the propagator matrix

$$[G_{NC}(Q^2)]_{0,N+1} = \frac{e^2 M_Z^2}{Q^2(Q^2 + M_Z^2)}\left[\prod_{z=1}^{N}\frac{\mathsf{m}^2_{Zz}}{Q^2 + \mathsf{m}^2_{Zz}}\right],$$
$$[G_{NC}(Q^2)]_{1,N+1} = \frac{e^2 M_Z^2}{Q^2(Q^2 + M_Z^2)}\left[\frac{Q^2 + \tilde{\mathsf{m}}^2}{\tilde{\mathsf{m}}^2}\right] \times \left[\prod_{z=1}^{N}\frac{\mathsf{m}^2_{Zz}}{Q^2 + \mathsf{m}^2_{Zz}}\right]. \qquad (4.1)$$

Combining these results, we find

$$[G_{NC}(Q^2)]_{WY} = \frac{e^2 M_Z^2}{Q^2(Q^2 + M_Z^2)}\left[1 + x_1\frac{Q^2}{\tilde{\mathsf{m}}^2}\right] \times \left[\prod_{z=1}^{N}\frac{\mathsf{m}^2_{Zz}}{Q^2 + \mathsf{m}^2_{Zz}}\right]. \qquad (4.2)$$

Given Eqs. (3.21) and (3.25), we may expand the final product in this expression and find

$$[G_{NC}(Q^2)]_{WY} = \frac{e^2 M_Z^2}{Q^2(Q^2 + M_Z^2)}\left[1 + Q^2\left(\frac{x_1}{\tilde{\mathsf{m}}^2} - \Sigma_Z\right)\right]. \qquad (4.3)$$

If we take

$$x_1 = \frac{\Sigma_Z}{\Sigma_{[0,1)}} = \tilde{\mathsf{m}}^2\Sigma_Z, \qquad (4.4)$$

we have that (in this momentum range) this correlation function equals its standard model value to leading order,

$$[G_{NC}(Q^2)]_{WY} \equiv [G_{NC}(Q^2)]^{\rm SM}_{WY}. \tag{4.5}$$

Next, we compute $[\xi_Z]_{WY}$, from which we may directly extract αS. The residue decomposes like the correlation function

$$[\xi_Z]_{WY} = x_0[\xi_Z]_{0,N+1} + x_1[\xi_Z]_{1,N+1}, \tag{4.6}$$

where the subscripts on the right-hand side of the equation denote the residue of the pole of the corresponding propagator matrix element. From Eq. (4.1), we find

$$\begin{aligned}[\xi_Z]_{0,N+1} &= -e^2[1 + M_Z^2\Sigma_Z],\\ [\xi_Z]_{1,N+1} &= -e^2[1 + M_Z^2(\Sigma_Z - \Sigma_{[0,1)})].\end{aligned} \tag{4.7}$$

Combining these results, we find

$$[\xi_Z]_{WY} = -e^2[1 + M_Z^2(\Sigma_Z - x_1\Sigma_{[0,1)})]. \tag{4.8}$$

The form of the four-fermion weak interaction amplitudes of Eqs. (3.19) and (3.20) implies [7]

$$\frac{1}{e^2}[\xi_Z]_{WY} = -1 - \frac{\alpha}{4s_Z^2c_Z^2}S, \tag{4.9}$$

and hence we find

$$\alpha S = 4s_Z^2c_Z^2M_Z^2(\Sigma_Z - x_1\tilde{\mathsf{m}}^{-2}). \tag{4.10}$$

Now it is clear that the same "tuning" of the localization of the fermion in conjunction with the heavy Z-boson mass matrix that causes $[G_{NC}(Q^2)]_{WY}$ to have its standard model form at low momentum likewise makes αS small. In fact, if Eq. (4.4) is satisfied, then $\alpha S \simeq 0$.

Using Eq. (3.18), we may rewrite this result in the form

$$\alpha S = 4s_Z^2c_Z^2M_Z^2(\Sigma_Z - x_1\Sigma_{p=1}), \tag{4.11}$$

which agrees with the results of [7] when $x_0 = 1$ or $x_1 = 1$, and smoothly interpolates between these extremes.

Finally, note that, in order for αS to be small, we need

$$x_1\frac{M_W^2}{\tilde{\mathsf{m}}^2} = M_W^2\Sigma_Z \ll 1, \tag{4.12}$$

and the limit of Eq. (3.25) is directly related to that of Eq. (3.21).

V. $[G_{NC}(Q^2)]_{YY}$, $[\xi_Z]_{YY}$ AND αT

Next, consider the correlation function $[G_{NC}(Q^2)]_{YY}$. Given the structure of the moose in Fig. 1 and the form of the fermion couplings in Eq. (3.1), we see that the delocalization of the fermions is irrelevant in this case—we get the same result [7] as in the case of the simplest case I model:

$$\begin{aligned}[G_{NC}(Q^2)]_{YY} = {}& \frac{e^2M_Z^2(Q^2 + M_W^2)}{Q^2M_W^2(Q^2 + M_Z^2)}\left[\prod_{w=1}^{N}\frac{Q^2 + \mathsf{m}_{Ww}^2}{\mathsf{m}_{Ww}^2}\right]\\ &\times\left[\prod_{z=1}^{N}\frac{\mathsf{m}_{Zz}^2}{Q^2 + \mathsf{m}_{Zz}^2}\right].\end{aligned} \tag{5.1}$$

Expanding for low Q^2 [see Eq. (3.21)] we find, to this order,

$$\begin{aligned}[G_{NC}(Q^2)]_{YY} &= \frac{e^2M_Z^2(Q^2 + M_W^2)}{Q^2M_W^2(Q^2 + M_Z^2)}[1 + Q^2(\Sigma_W - \Sigma_Z)]\\ &= [G_{NC}(Q^2)]^{\rm SM}_{YY},\end{aligned} \tag{5.2}$$

where the last equality follows from Eq. (3.23) and where $[G_{NC}(Q^2)]^{\rm SM}_{YY}$ denotes the tree-level standard model value in terms of e^2, M_W^2, and M_Z^2 .

The residue is likewise the same as in the simplest case I model:

$$[\xi_Z]_{YY} = \frac{e^2(M_Z^2 - M_W^2)}{M_W^2}[1 + M_Z^2(\Sigma_Z - \Sigma_W)]. \tag{5.3}$$

Therefore, using the results of [7], we find

$$\alpha T = s_Z^2M_Z^2(\Sigma_Z - \Sigma_W) \simeq 0, \tag{5.4}$$

independent of the value of x_0. The last equality follows from Eq. (3.23) (i.e. from working in the limit $g_{N+1}^2 \ll 1$).

VI. $[G_{CC}(Q^2)]_{WW}$, $[\xi_W]_{WW}$, AND $\alpha\delta$

Finally, to compute $\alpha\delta$ we must compute a WW correlation function. For simplicity, we will consider the charged-current correlation function $[G_{CC}(Q^2)]_{WW}$. We may do so by recalling that the matrix $G_{CC}(Q^2)$ is defined by

$$[G_{CC}(Q^2)]_{i,j} \equiv g_ig_j[(Q^2 + M_W^2)^{-1}]_{i,j}. \tag{6.1}$$

The correlation function of J_μ^+ with J_ν^- is therefore proportional to

$$x_0^2[G_{CC}(Q^2)]_{0,0} + 2x_0x_1[G_{CC}(Q^2)]_{0,1} + x_1^2[G_{CC}(Q^2)]_{1,1}. \tag{6.2}$$

To make progress, we relate the various propagator elements to one another. Consider Eq. (6.1) as a matrix equation

$$G_{CC}(Q^2) = G\cdot\frac{\mathcal{I}}{Q^2 + M_W^2}\cdot G, \tag{6.3}$$

where G is the matrix of gauge coupling constants and $\mathcal{I}$ denotes the identity matrix in gauge space. From this, we immediately see that we have the matrix relation

$$(Q^2 + M_W^2)\cdot G^{-1}\cdot G_{CC}(Q^2)\cdot G^{-1} \equiv \mathcal{I}. \tag{6.4}$$

Applying this relation explicitly to the first row of the matrix $(Q^2 + M_W^2)$ and the first two columns of the matrix $G_{CC}(Q^2)$, we find the relations[5]

$$[G_{CC}(Q^2)]_{0,1} = \frac{\tilde{m}^2}{Q^2 + \tilde{m}^2}[G_{CC}(Q^2)]_{1,1}, \tag{6.5}$$

and

$$[G_{CC}(Q^2)]_{0,0} = \frac{g_0^2(1 + \frac{f_1^2}{4}[G_{CC}(Q^2)]_{0,1})}{Q^2 + \tilde{m}^2}. \tag{6.6}$$

Using these results, we find

$$[G_{CC}(Q^2)]_{WW} = \left(1 + x_1\frac{Q^2}{\tilde{m}^2}\right)^2[G_{CC}(Q^2)]_{0,0} - \frac{8x_1}{f_1^2} + \frac{4x_1^2}{f_1^2}\left(1 - \frac{Q^2}{\tilde{m}^2}\right). \tag{6.7}$$

Given the limit of Eq. (3.25), for the momenta of interest this reduces to

$$[G_{CC}(Q^2)]_{WW} = \left(1 + 2x_1\frac{Q^2}{\tilde{m}^2}\right)[G_{CC}(Q^2)]_{0,0} - \frac{8x_1}{f_1^2} + \frac{4x_1^2}{f_1^2}. \tag{6.8}$$

We can rearrange this to isolate the pole at $Q^2 = -M_W^2$ from the nonpole pieces of the correlation function:

$$\begin{aligned}[G_{CC}(Q^2)]_{WW} &= \left(1 - 2x_1\frac{M_W^2}{\tilde{m}^2}\right)[G_{CC}(Q^2)]_{0,0} \\ &\quad + \frac{2x_1}{\tilde{m}^2}(Q^2 + M_W^2)[G_{CC}(Q^2)]_{0,0} \\ &\quad - \frac{4x_1}{F^2}\left(\frac{M_W^2}{\tilde{m}^2}\right)(2 - x_1),\end{aligned} \tag{6.9}$$

where we have used Eq. (3.24) to simplify the last term.

From the pole term (first term) of Eq. (6.9) we see that the residue of the charged-current correlation function at $Q^2 = -M_W^2$ is

$$[\xi_W]_{WW} = \left(1 - 2x_1\frac{M_W^2}{\tilde{m}^2}\right)[\xi_W]_{0,0}. \tag{6.10}$$

Applying the calculations presented in [7], we observe that

$$\begin{aligned}[\xi_W]_{0,0} &= \frac{e^2M_Z^2}{M_Z^2 - M_W^2}[1 + M_W^2(\Sigma_Z + \Sigma_W)] \\ &= [\xi_W]^{\rm SM}[1 + 2M_W^2\Sigma_Z],\end{aligned} \tag{6.11}$$

where the last equality follows from Eq. (3.23), and $[\xi_W]^{\rm SM}$ denotes the tree-level standard model value of the residue expressed in terms of $M_{W,Z}^2$. Therefore, we find from Eq. (6.10) that

$$[\xi_W]_{WW} = \left(1 - 2x_1\frac{M_W^2}{\tilde{m}^2} + 2M_W^2\Sigma_Z\right)[\xi_W]^{\rm SM}. \tag{6.12}$$

For $x_1 = \tilde{m}^2\Sigma_Z$ (i.e., for $\alpha S = 0$), the residue of the pole equals the standard model value. This is consistent with the form of Eq. (3.20).

While the residue of the W pole is given by its standard model value, the nonpole terms in Eq. (6.9) give rise to a nonzero value of $\alpha\delta$. From the analyses presented in [7],

$$[G_{CC}(Q^2)]_{0,0} = \frac{4M_W^2}{F^2[Q^2 + M_W^2]}\left[\prod_{w=1}^{N}\frac{m_{Ww}^2}{Q^2 + m_{Ww}^2}\right] \times\left[\prod_{r=1}^{N}\frac{Q^2 + m_r^2}{m_r^2}\right]. \tag{6.13}$$

Expanding the product for the momenta of interest, this may be written

$$\begin{aligned}[G_{CC}(Q^2)]_{0,0} &= \frac{4M_W^2}{F^2[Q^2 + M_W^2]}[1 + Q^2(\Sigma_r - \Sigma_W)] \\ &\approx \frac{4M_W^2}{F^2[Q^2 + M_W^2]},\end{aligned} \tag{6.14}$$

where the last equality follows from Eq. (3.23). Comparing the nonpole terms in Eq. (6.9) with the form of the matrix element Eq. (3.20), we therefore calculate

$$\sqrt{2}G_F\frac{\alpha\delta}{s^2c^2} = \frac{4x_1^2}{F^2}\left(\frac{M_W^2}{\tilde{m}^2}\right). \tag{6.15}$$

However,

$$\sqrt{2}G_F \equiv \frac{1}{4}[G_{CC}(Q^2 = 0)]_{WW} \tag{6.16}$$

so from Eq. (6.8), again using Eqs. (3.17) and (3.24), we see that

$$\begin{aligned}\sqrt{2}G_F &= \frac{1}{F^2} - \frac{(2 - x_1)x_1}{f_1^2} \approx \frac{1}{F^2}\left[1 - \frac{(2 - x_1)x_1M_W^2}{\tilde{m}^2}\right] \\ &= \frac{1}{F^2}\left[1 + \mathcal{O}\left(\frac{x_1M_W^2}{\tilde{m}^2}\right)\right].\end{aligned} \tag{6.17}$$

Using this in Eq. (6.15) we find

$$\frac{\alpha\delta}{4s^2c^2} = x_1^2\frac{M_W^2}{\tilde{m}^2}. \tag{6.18}$$

If we employ Eq. (3.18), this can be rewritten as

$$\frac{\alpha\delta}{4s^2c^2} = x_1^2M_W^2\Sigma_{p=1}, \tag{6.19}$$

which agrees with the results of [7] for $x_0 = 1$ or $x_1 = 1$ and smoothly interpolates between them.

[5]The propagator matrix elements $[G_{CC}(Q^2)]_{0,1}$ and $[G_{CC}(Q^2)]_{0,0}$ do not have poles at $Q^2 = -\tilde{m}^2$, as might be inferred from the form of Eqs. (6.5) and (6.6). Rather, these potential poles are canceled by zeros of the numerators in these expressions.

When we choose the amount of delocalization to ensure that αS vanishes, $x_1 = \tilde{m}^2\Sigma_Z$, we find

$$\frac{\alpha\delta}{4s^2c^2} = x_1 M_W^2 \Sigma_Z. \tag{6.20}$$

Moreover, as argued previously [7], preserving the unitarity of longitudinal W boson scattering requires that $M_W^2\Sigma_Z \geq 4 \times 10^{-3}$. The results of [12] imply[6] that experiment currently imposes the upper bound $\alpha\delta/4s^2c^2 < 1 \times 10^{-3}$ at 95% C.L. Hence we must have

$$x_1 \leq \frac{1}{4}, \tag{6.21}$$

and the amount of delocalization is bounded to be less than of order 25%.

VII. BEYOND EXTRA DIMENSIONS

A. Reinterpreting fermion delocalization

The delocalized fermion coupling in deconstructed Higgsless models, Eq. (3.1), may also be written using the Goldstone-boson fields of the moose in Fig. 1. Consider the current operator

$$\mathrm{Tr}\left(\frac{\sigma^a}{2} U_1^\dagger i D_\mu U_1\right) \to +\frac{1}{2}(A^a_{0\mu} - A^a_{1\mu}), \tag{7.1}$$

where the σ are the Pauli matrices, D_μ is the covariant derivative

$$iD_\mu U_1 = i\partial_\mu U_1 + \frac{\vec{A}_{0\mu}\cdot\vec{\sigma}}{2}U_1 - U_1\frac{\vec{A}_{1\mu}\cdot\vec{\sigma}}{2}, \tag{7.2}$$

consistent with Eq. (3.1), and where we have specified the form of this operator in unitary gauge, where all the link fields $U_j \equiv \mathcal{I}$. In this language, we see that the fermions' weak couplings in Eq. (3.1) may be written

$$\vec{J}_L^{\,\mu} \cdot \left[\vec{A}^0_\mu - 2x_1 \mathrm{Tr}\left(\frac{\vec{\sigma}}{2} U_1^\dagger i D_\mu U_1\right)\right]. \tag{7.3}$$

From this point of view, the fermions are charged only under $SU(2)_0$ and the apparent delocalization comes about from couplings to the Goldstone-boson fields.[7]

Note that, in the gauge-boson normalization we are using, the linear combination of gauge fields $A^a_{0\mu} - A^a_{1\mu}$ are strictly orthogonal to the photon

$$A^\gamma_\mu \propto A^3_{0\mu} + A^3_{1\mu} + \cdots + A^3_{N+1\mu}. \tag{7.4}$$

Hence, the couplings of Eq. (7.3) result in a modification of the Z and W couplings whose size depends on the x_1 and the admixture of $A_0 - A_1$ in the mass eigenstate W and Z fields. *But the couplings of Eq.* (7.3) *do not modify the photon coupling.*

B. Technicolor

We have seen that fermion delocalization, on the one hand, affects αS, and, on the other, can be rewritten as the fermions coupling to the Goldstone-boson currents. We can apply the idea of fermions' coupling to Goldstone bosons directly to technicolor—a two-site model—which has no extra-dimensional interpretation. Consider the two-site model of Fig. 2, with fermion couplings[8]

$$\mathcal{L}_f = \vec{J}_L^\mu \cdot \left[\vec{A}^0_\mu - 2x_1 \mathrm{Tr}\left(\Sigma^\dagger \frac{\vec{\sigma}}{2} i D_\mu \Sigma\right)\right] + J_Y^\mu A^1_\mu, \tag{7.5}$$

where Σ is the unitary matrix representing the three eaten Goldstone bosons, and the $\vec{\sigma}$ are the Pauli matrices. Following [42], we find that in unitary gauge

$$\begin{aligned} &2x_1 \vec{J}_L^\mu \cdot \mathrm{Tr}\left(\Sigma^\dagger \frac{\vec{\sigma}}{2} i D_\mu \Sigma\right) \\ &\quad \to -2x_1\left[\frac{e}{\tilde{s}\,\tilde{c}} Z^\mu J^3_\mu + \frac{e}{\tilde{s}\sqrt{2}}(W^{+\mu}J^-_\mu + W^{-\mu}J^+_\mu)\right], \end{aligned} \tag{7.6}$$

where

$$g_0 = \frac{e}{\tilde{s}}, \qquad g_1 = \frac{e}{\tilde{c}}. \tag{7.7}$$

Hence, we find the overall Z and W couplings

$$\frac{e}{\tilde{s}\,\tilde{c}} Z^\mu[(1-2x_1)J^3_\mu - \tilde{s}^2 J^Q_\mu], \tag{7.8}$$

$$\frac{e}{\sqrt{2}\tilde{s}}(1-2x_1)[W^{+\mu}J^-_\mu + W^{-\mu}J^+_\mu]. \tag{7.9}$$

Comparing with Eqs. (3.19) and (3.20) we find

$$\tilde{s}^{\,2} = s^2(1-2x_1), \qquad \alpha\Delta S \approx -8s^2 x_1. \tag{7.10}$$

As anticipated, the Goldstone-boson operator in Eq. (7.5) can shift αS. In fact, it will shift αS in a negative direction (since x_1 is positive) just as occurs in Eq. (4.10).

In a technicolor model this effect could be used to cancel the positive QCD-size value of αS arising [36,43,44] from the L_{10} operator. It is also amusing to note that the sign of x_1 arising from the extended technicolor coupling (ETC) operators considered in [42] is positive. If the operator of Eq. (7.5) arises from ETC exchange, that reference found (note that the convention for the covariant derivative differs in that reference)

$$x_1 = \frac{\xi^2}{4}\frac{g^2_{\mathrm{ETC}} v^2}{M^2_{\mathrm{ETC}}}, \tag{7.11}$$

[6] When $\alpha S = 0 = (\Delta\rho - \alpha T)$, from Eq. (1.1) we see that $\hat{S} = \alpha\delta/4s^2c^2$.

[7] This also generalizes naturally to models with multisite delocalization.

[8] This kind of operator was previously considered in Refs. [39–42], the first of these prior to the definition of αS and the last considering only flavor-dependent effects. Note that there is only one $SU(2)$ group.

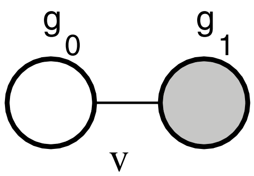

FIG. 2. Simple two-site moose diagram corresponding to the global symmetry structure of the one-Higgs doublet standard model or the simplest one-doublet technicolor model.

where $g_{\rm ETC}$ and $M_{\rm ETC}$ are the extended technicolor coupling and gauge-boson mass, $v \simeq 246$ GeV, and ξ is a model-dependent Clebsch-Gordon coefficient. The canonical QCD-like technicolor estimate gives $S_{\rm TC} = \mathcal{O}(0.5)$. If we require the sum of the canonical contribution plus that arising from Eq. (7.10) to vanish, we find $|x_1| \simeq 2 \times 10^{-3}$, and hence

$$\frac{M_{\rm ETC}}{\xi g_{\rm ETC}} \simeq 3\ \text{TeV}. \tag{7.12}$$

In an ETC model, one would also expect contributions to $\alpha\delta$ (from ETC exchange) of the same order—which implies there must be a Clebsch of order a few to suppress $\alpha\delta$ relative to x_1 [12]. One could imagine, for example, a model with flavor-independent left-handed low-scale ETC interactions (with light quark masses suppressed by high-scale right-handed interactions).

VIII. EXAMPLES OF DELOCALIZED DECONSTRUCTED HIGGSLESS MODELS

To illustrate the ideas discussed in the earlier sections of the paper, we now study a linear moose model with 4 sites and 3 links (Fig. 3), a model small enough to be easily solved numerically without approximations. We will calculate the tree-level masses and residues exactly and confirm that our previous analytic calculations based on the approximations of Eqs. (3.22) and (3.25) capture the essential features of models with one-site delocalization.

Starting from this $[SU(2)]^3 \times U(1)$ gauge structure, we introduce a chiral fermion ψ_{0L} [assumed to be a doublet of $SU(2)_0$], and a Dirac fermion $\psi_1 = \psi_{1L} + \psi_{1R}$ [doublet of $SU(2)_1$]. Both ψ_{0L} and ψ_1 are assumed to have the same weak hypercharge Y_ψ. The fermion sector of this model is then given by the Lagrangian,

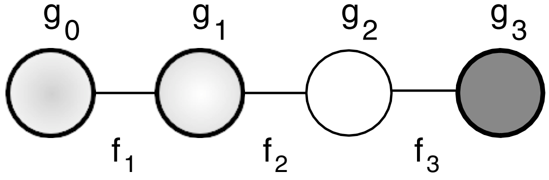

FIG. 3. The model analyzed in the explicit numerical calculation. Sites 0 to 2 are $SU(2)$ gauge groups, while site 3 is $U(1)$. Fermions are coupled to sites 0 and 1 (weak isospin), and to site 3 (weak hypercharge), as denoted by the thick circles.

$$\begin{aligned}\mathcal{L}_{\rm fermion} = {}& \bar\psi_{0L}\Big(i\partial\!\!\!/ + \frac{\tau^a}{2} A\!\!\!/_0^a + Y_\psi A\!\!\!/_3\Big)\psi_{0L} \\ &+ \bar\psi_{1L}\Big(i\partial\!\!\!/ + \frac{\tau^a}{2} A\!\!\!/_1^a + Y_\psi A\!\!\!/_3\Big)\psi_{1L} \\ &+ \bar\psi_{1R}\Big(i\partial\!\!\!/ + \frac{\tau^a}{2} A\!\!\!/_1^a + Y_\psi A\!\!\!/_3\Big)\psi_{1R}.\end{aligned} \tag{8.1}$$

The fermion mass term consistent with the gauge symmetry is given by

$$\mathcal{L}_{\rm mass} = (\bar\psi_{0L}, \bar\psi_{1L})\begin{pmatrix} y_\psi f_1 U_1 \\ M_\psi \end{pmatrix}\psi_{1R} + \text{H.c.} \tag{8.2}$$

After the gauge symmetry breaking, ψ_{1R} and

$$\psi_L^{(1)} = s_\psi \psi_{0L} + c_\psi \psi_{1L} \tag{8.3}$$

form a Dirac fermion and become massive; we identify this as a KK mode. There also remains a massless fermion

$$\psi_L^{(0)} = c_\psi \psi_{0L} - s_\psi \psi_{1L}, \tag{8.4}$$

where

$$c_\psi \equiv \frac{M_\psi}{\sqrt{y_\psi^2 f_1^2 + M_\psi^2}}, \qquad s_\psi \equiv \frac{y_\psi f_1}{\sqrt{y_\psi^2 f_1^2 + M_\psi^2}}, \tag{8.5}$$

which we identify as the standard model fermion. Then $\psi_L^{(0)}$ couples to the gauge fields as

$$\mathcal{L}_{\rm fermion} = \bar\psi_L^{(0)}\Big(i\partial\!\!\!/ + x_0\frac{\tau^a}{2} A\!\!\!/_0^a + x_1\frac{\tau^a}{2} A\!\!\!/_1^a + Y_\psi A\!\!\!/_3\Big)\psi_L^{(0)} + \cdots, \tag{8.6}$$

where $x_0 = c_\psi^2$ and $x_1 = s_\psi^2$.

In our phenomenological calculations, we use α, G_F, and M_Z to specify the input parameters of the standard model.[9] The specific values used are [45] $\alpha^{-1} = 128.91 \pm 0.02$, $M_Z = 91.1876 \pm 0.0021$ GeV, and $G_F = 1.166\,37 \times 10^{-5}$ GeV^{-2}. The Weinberg angle in this scheme is defined by

$$s_Z^2 c_Z^2 \equiv \frac{e^2}{4\sqrt{2} G_F M_Z^2}, \qquad c_Z^2 \equiv 1 - s_Z^2, \tag{8.7}$$

yielding $s_Z^2 = 0.231\,08 \pm 0.000\,05$.

Our four-site linear moose model with one delocalized fermion can be specified by 8 parameters: f_i ($i = 1, 2, 3$), g_i ($i = 0, 1, 2, 3$) and x_1^2. Three combinations of these parameters have values set by the inputs α, G_F, and M_Z.

[9] Note that the tree-level value of M_W in this scheme ($M_W|_{\rm tree} \equiv c_Z M_Z = 79.9607$ GeV) differs from the observed value ($M_W|_{\rm exp} = 80.425 \pm 0.038$ GeV), indicating the importance of a one-loop radiative correction at 1% level. In this paper, however, we restrict ourselves to tree level. We thus denote $M_W^{\rm SM} \equiv M_W|_{\rm tree}$ in our calculations, and compare all correlation functions to the corresponding tree-level standard model results.

For instance,

$$\frac{1}{4\pi\alpha} = \sum_{i=0}^{3} \frac{1}{g_i^2}, \tag{8.8}$$

and

$$4\sqrt{2}G_F = [G_{CC}(Q^2 = 0)]_{WW}, \tag{8.9}$$

where one applies Eq. (3.6) together with

$$[G_{CC}(Q^2 = 0)]_{0,0} = \sum_{i=1,2,3} \frac{4}{f_i^2},$$

$$[G_{CC}(Q^2 = 0)]_{0,1} = [G_{CC}(Q^2 = 0)]_{1,1} = \sum_{i=2,3} \frac{4}{f_i^2}. \tag{8.10}$$

Requiring $S = 0$ sets the value of one more combination, as in Eq. (4.12). In order to specify the remaining parameters, we adopt three ansatzes

$$f_2 = f_3, \quad g_1 = g_2 = 4. \tag{8.11}$$

The ansatz $f_2 = f_3$ allows us to maximize the delay of the onset of unitarity violation in longitudinal W scattering. The large values of g_1 and g_2 are taken so as to push up the mass of the gauge-boson KK modes. Combining the four requirements from (α, G_F, M_Z, S) with the three ansatzes, only one free parameter, which we identify as f_1, is left in the four-site model.

We have analyzed the four-site model with three sample values of the single free parameter: $f_1 = 300$ GeV (set 1), $f_1 = 1000$ GeV (set 2) and $f_1 = 2000$ GeV (set 3). Once f_1 is chosen, the other f_i, the g_i and x_1 have values given in Table I, as set by the four inputs and three ansatzes. The masses listed as outputs in the Table were calculated by diagonalizing the gauge-boson mass-squared matrix numerically.

The calculated values of M_W in sets 1 and 2 agree with the tree-level standard model value within the uncertainty of $M_W|_{\mathrm{exp}}$ about 0.038 GeV. Hence the measured value of M_W does not currently exclude either set 1 or 2. The calculated value of M_W in set 3 deviates from the tree-level standard model value by about 1.4σ; set 3 is therefore marginally excluded.

A. Correlation functions

To explore the expectations that the electroweak correlation functions will resemble their standard model counterparts at low momentum, we calculated their values over the LEP energy range $\sqrt{-Q^2} = 90$–200 GeV, and compared the tree-level results in the moose model to the tree-level results in the standard model. We computed $[G_{NC}(Q^2)]_{WY}$ for all three sets of parameters using expression (4.2) and found no discernible deviation of the ratio $[G_{NC}(Q^2)]_{WY}^{\mathrm{Higgsless}}/[G_{NC}(Q^2)]_{WY}^{\mathrm{SM}}$ from one. This is consistent with the fact that the model parameters were chosen to make αS vanish. Small deviations from one were found in the corresponding ratios for $[G_{NC}(Q^2)]_{YY,WW}$.

Figure 4 depicts the behavior of $[G_{NC}(Q^2)]_{YY}/[G_{NC}(Q^2)]_{YY}^{\mathrm{SM}}$ as calculated using Eq. (5.1). Set 1, shown by the lowest curve in the figure, is indistinguishable from the standard model. The middle curve shows the ratio for the moose with set 2 parameters; the upper curve shows the effect of using set 3 parameters instead. For sets 2 and 3, the deviation from the standard model value is quite small; the visible deviation near $\sqrt{-Q^2} \simeq 90$ GeV comes from the difference between $c_Z M_Z$ and M_W.

The form of the correlation function $[G_{NC}(Q^2)]_{WW}$ is derived by starting from Eq. (3.6) and working in parallel with the arguments in Sec. VI and Ref. [7] to find

$$[G_{NC}(Q^2)]_{0,i} = \frac{e^2 M_Z^2}{Q^2(Q^2 + M_Z^2)} \left[\prod_{z=1,2} \frac{\mathsf{m}_z^2}{Q^2 + \mathsf{m}_z^2}\right] \times \frac{\det[Q^2 + M_{(i,3]}^2]}{\det[M_{(i,3]}^2]}, \tag{8.12}$$

TABLE I. Model parameters.

	Set 1	Set 2	Set 3
Inputs			
f_1	300 GeV	1000 GeV	2000 GeV
$f_2 = f_3$	591.850 GeV	356.303 GeV	348.922 GeV
g_0	0.657 164	0.664 421	0.663 478
$g_1 = g_2$	4.0	4.0	4.0
g_3	0.357 650	0.356 505	0.356 651
x_1	0.014 771	0.139 231	0.480 892
Calculated physical masses			
M_W	79.9599 GeV	79.9486 GeV	79.9080 GeV
m_{Z1}	892.459 GeV	976.990 GeV	983.725 GeV
m_{W1}	888.827 GeV	975.913 GeV	982.737 GeV
m_{Z2}	1944.08 GeV	2162.17 GeV	4114.49 GeV
m_{W2}	1943.39 GeV	2162.17 GeV	4144.49 GeV

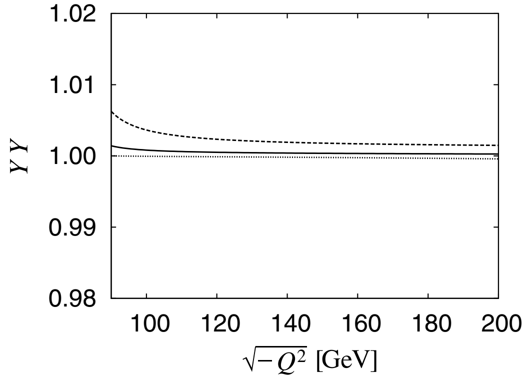

FIG. 4. $[G_{NC}(Q^2)]_{YY}/[G_{NC}(Q^2)]^{\rm SM}_{YY}$ for the LEP energy range. From lowest to highest, the curves are for the sets 1, 2, and 3 parameters. Set 1 is indistinguishable from the standard model in this plot.

$$[G_{NC}(Q^2)]_{1,1} = \left[1 + \frac{Q^2}{\tilde{\mathsf{m}}^2}\right][G_{NC}(Q^2)]_{0,1}. \tag{8.13}$$

We calculate the eigenvalues of matrix $M^2_{(0,3]}$ in the four-site model to be

$$\text{set 1: } 43.4066\ \text{GeV}, \quad 890.794\ \text{GeV}, \quad 1943.92\ \text{GeV}, \tag{8.14}$$

$$\text{set 2: } 43.4996\ \text{GeV}, \quad 972.319\ \text{GeV}, \quad 2140.13\ \text{GeV}, \tag{8.15}$$

$$\text{set 3: } 43.6216\ \text{GeV}, \quad 982.737\ \text{GeV}, \quad 4114.49\ \text{GeV}, \tag{8.16}$$

and those of matrix $M^2_{(1,3]}$ are found to be

$$\text{set 1: } 74.7636\ \text{GeV}, \quad 1675.68\ \text{GeV}, \tag{8.17}$$

$$\text{set 2: } 44.8651\ \text{GeV}, \quad 1008.779\ \text{GeV}, \tag{8.18}$$

$$\text{set 3: } 43.9536\ \text{GeV}, \quad 987.883\ \text{GeV}. \tag{8.19}$$

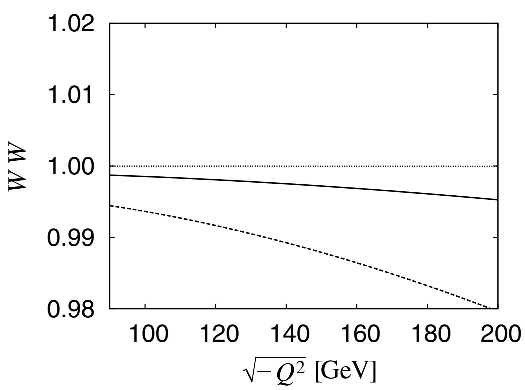

FIG. 5. $[G_{NC}(Q^2)]_{WW}/[G_{NC}(Q^2)]^{\rm SM}_{WW}$ for the LEP energy range. From highest to lowest, the curves are for the sets 1, 2, and 3 parameters. Set 1 is indistinguishable from the standard model in this plot.

The $[G_{NC}(Q^2)]_{WW}$ results for sets 1, 2, and 3 are depicted in the upper, middle, and lower curves of Fig. 5. Set 1 is, again, indistinguishable from the standard model. For the set 2 parameters, the deviation of the correlation function from its standard model form is less than 0.5% even at $\sqrt{-Q^2} = 200$ GeV; this choice of parameters seems to be phenomenologically acceptable. For set 3, the deviation is about 2% at $\sqrt{-Q^2} = 200$ GeV, which is too large to be phenomenologically acceptable.

B. Electroweak corrections

By construction, we expect that the electroweak corrections other than $\alpha\delta$ will be suppressed for any of our sample sets of parameters. Because the model is case I [7], $\Delta\rho = 0$; because g_{N+1} is small (3.22) , $\alpha T \approx 0$; the value of x_1 was explicitly chosen (4.12) to make $\alpha S \approx 0$. This turns out to be the case; numerical evaluation shows $|\alpha S| \lesssim 10^{-5}$, $|\alpha T| \lesssim 10^{-5}$, $|\alpha U| \lesssim 10^{-5}$.

However, the value of $\alpha\delta$ is not automatically small enough to agree with constraints set by data. Set 1 has the smallest value of x_1, and the corresponding value of $\alpha\delta$ is zero to within the limits of numerical accuracy. For set 2, the experimental upper bound [12] of order 0.001 is satisfied by the quantity

$$\frac{\alpha\delta}{4s_Z^2c_Z^2} = 1 - \frac{[\xi_W]_{WW}}{4\sqrt{2}G_F M_W^2} = 0.70 \times 10^{-3}. \tag{8.20}$$

Note that the approximate value for $\alpha\delta$ from Eq. (6.20) is consistent with the exact result above: the difference is precisely the size of the terms neglected in the approximation. For set 3, on the other hand, $\alpha\delta$ lies above the experimental bound

$$\frac{\alpha\delta}{4s_Z^2c_Z^2} = 3.04 \times 10^{-3}. \tag{8.21}$$

In other words, choosing the amount of delocalization to guarantee that the oblique correction αS is small does not guarantee that the universal nonoblique correction $\alpha\delta$ will be of acceptable size. The first requires x_1 to be a function of the couplings and f constants; the second places an absolute upper bound on the value of x_1. In our four-site model, the most significant effect of the larger value of f_1 for set 3 was to drive x_1 larger—which pushed $\alpha\delta$ too high.

IX. CONCLUSIONS

In this note we have calculated the form of electroweak corrections in deconstructed Higgsless models for the case of a fermion whose weak properties arise from two adjacent $SU(2)$ groups on the deconstructed lattice. We have shown that, as recently proposed in the continuum [31,32], it is possible for the value of the electroweak parameter αS to be small in such a model. Working in the deconstructed limit we have also directly evaluated the size of $\alpha\delta$, arising off-Z-pole from the exchange of Kaluza-Klein modes [9]. This has not previously been evaluated in the continuum. In one-site delocalized Higgsless models with small values of αS, we showed that the amount of delocalization is bounded to be less than of order 25% at 95% C.L. due to the simultaneous need to ensure unitarization of $W_L W_L$ scattering and to provide a value of $\alpha\delta$ that agrees with experiment. We have discussed the relation of these calculations to our previous calculations in deconstructed Higgsless models [7], and to models of extended technicolor. Finally, we presented numerical results for a four-site model, illustrating our analytic calculations. In a subsequent publication [33,34], we will generalize our discussion to multisite delocalization and discuss the effects of fermion delocalization in the continuum.

ACKNOWLEDGMENTS

R. S. C. and E. H. S. are supported in part by the U.S. National Science Foundation under No. PHY-0354226. M. K. acknowledges support by the 21st Century COE Program of Nagoya University provided by JSPS (15COEG01). M. T.'s work is supported in part by the JSPS Grant-in-Aid for Scientific Research No. 16540226. H. J. H. is supported by the U.S. Department of Energy Grant No. DE-FG03-93ER40757.

[1] C. Csaki, C. Grojean, H. Murayama, L. Pilo, and J. Terning, Phys. Rev. D **69**, 055006 (2004).
[2] R. Sekhar Chivukula, D. A. Dicus, and H.-J. He, Phys. Lett. B **525**, 175 (2002).
[3] R. S. Chivukula and H.-J. He, Phys. Lett. B **532**, 121 (2002).
[4] R. S. Chivukula, D. A. Dicus, H.-J. He, and S. Nandi, Phys. Lett. B **562**, 109 (2003).
[5] H. J. He, hep-ph/0412113.
[6] P. W. Higgs, Phys. Lett. **12**, 132 (1964).
[7] R. Sekhar Chivukula, E. H. Simmons, H.-J. He, M. Kurachi, and M. Tanabashi, Phys. Rev. D **71**, 035007 (2005).
[8] R. S. Chivukula, E. H. Simmons, H.-J. He, M. Kurachi, and M. Tanabashi, Phys. Rev. D **70**, 075008 (2004).
[9] R. S. Chivukula, E. H. Simmons, H.-J. He, M. Kurachi, and M. Tanabashi, Phys. Lett. B **603**, 210 (2004).
[10] N. Arkani-Hamed, A. G. Cohen, and H. Georgi, Phys. Rev. Lett. **86**, 4757 (2001).
[11] C. T. Hill, S. Pokorski, and J. Wang, Phys. Rev. D **64**, 105005 (2001).
[12] R. Barbieri, A. Pomarol, R. Rattazzi, and A. Strumia, Nucl. Phys. **B703**, 127 (2004).
[13] R. S. Chivukula, H.-J. He, J. Howard, and E. H. Simmons, Phys. Rev. D **69**, 015009 (2004).
[14] R. Casalbuoni, S. De Curtis, D. Dominici, and R. Gatto, Phys. Lett. **155B**, 95 (1985).
[15] R. Casalbuoni *et al.*, Phys. Rev. D **53**, 5201 (1996).
[16] R. Casalbuoni, S. De Curtis, and D. Dominici, Phys. Rev. D **70**, 055010 (2004).
[17] M. Bando, T. Kugo, S. Uehara, K. Yamawaki, and T. Yanagida, Phys. Rev. Lett. **54**, 1215 (1985).
[18] M. Bando, T. Kugo, and K. Yamawaki, Nucl. Phys. **B259**, 493 (1985).
[19] M. Bando, T. Fujiwara, and K. Yamawaki, Prog. Theor. Phys. **79**, 1140 (1988).
[20] M. Bando, T. Kugo, and K. Yamawaki, Phys. Rep. **164**, 217 (1988).
[21] M. Harada and K. Yamawaki, Phys. Rep. **381**, 1 (2003).
[22] C. Csaki, C. Grojean, L. Pilo, and J. Terning, Phys. Rev. Lett. **92**, 101802 (2004).
[23] Y. Nomura, J. High Energy Phys. 11 (2003) 050.
[24] R. Barbieri, A. Pomarol, and R. Rattazzi, Phys. Lett. B **591**, 141 (2004).
[25] H. Davoudiasl, J. L. Hewett, B. Lillie, and T. G. Rizzo, Phys. Rev. D **70**, 015006 (2004).
[26] R. Foadi, S. Gopalakrishna, and C. Schmidt, J. High Energy Phys. 03 (2004) 042.
[27] G. Burdman and Y. Nomura, Phys. Rev. D **69**, 115013 (2004).
[28] H. Davoudiasl, J. L. Hewett, B. Lillie, and T. G. Rizzo, J. High Energy Phys. 05 (2004) 015.
[29] J. L. Hewett, B. Lillie, and T. G. Rizzo, J. High Energy Phys. 10 (2004) 014.
[30] M. Perelstein, J. High Energy Phys. 10 (2004) 010.
[31] G. Cacciapaglia, C. Csaki, C. Grojean, and J. Terning, Phys. Rev. D **71**, 035015 (2005).
[32] R. Foadi, S. Gopalakrishna, and C. Schmidt, Phys. Lett. B **606**, 157 (2005).
[33] R. Sekhar Chivukula, E. H. Simmons, H. J. He, M. Kurachi, and M. Tanabashi, hep-ph/0504114.
[34] R. Sekhar Chivukula, E. H. Simmons, H.-J. He, M. Kurachi, and M. Tanabashi (unpublished).
[35] H. Georgi, Nucl. Phys. **B266**, 274 (1986).
[36] M. E. Peskin and T. Takeuchi, Phys. Rev. D **46**, 381 (1992).
[37] G. Altarelli and R. Barbieri, Phys. Lett. B **253**, 161 (1991).
[38] G. Altarelli, R. Barbieri, and S. Jadach, Nucl. Phys. **B369**, 3 (1992).
[39] L. J. Hall and S. F. King, Nucl. Phys. **B287**, 551 (1987).
[40] R. S. Chivukula and H. Georgi, Phys. Rev. D **36**, 2102 (1987).
[41] L. Randall and R. S. Chivukula, Nucl. Phys. **B326**, 1 (1989).
[42] R. S. Chivukula, S. B. Selipsky, and E. H. Simmons, Phys. Rev. Lett. **69**, 575 (1992).
[43] M. Golden and L. Randall, Nucl. Phys. **B361**, 3 (1991).
[44] B. Holdom and J. Terning, Phys. Lett. B **247**, 88 (1990).
[45] S. Eidelman *et al.* (Particle Data Group), Phys. Lett. B **592**, 1 (2004).